

Article

The Dragon's Paralysing Spell: Evidence of Sodium and Calcium Ion Channel Binding Neurotoxins in Helodermatid and Varanid Lizard Venoms

James S. Dobson ¹, Richard J. Harris ¹, Christina N. Zdenek ¹, Tam Huynh ², Wayne C. Hodgson ², Frank Bosmans ³, Rudy Fourmy ⁴, Aude Violette ⁴ and Bryan G. Fry ^{1,*}

- ¹ Venom Evolution Lab, School of Biological Sciences, University of Queensland, St. Lucia, QLD 4072, Australia; j.dobson@uq.edu.au (J.S.D.); rharris2727@googlemail.com (R.J.H.); christinazdenek@gmail.com (C.N.Z.)
- ² Department of Pharmacology, Biomedicine Discovery Institute, Monash University, Clayton, VIC 3800, Australia; tlhuy3@student.monash.edu (T.H.); wayne.hodgson@monash.edu (W.C.H.)
- ³ Department of Basic and Applied Medical Sciences, Ghent University, 9000 Ghent, Belgium; Frank.Bosmans@ugent.be
- ⁴ Alphabiotoxine Laboratory sprl, Barberie 15, 7911 Montroeuil-au-Bois, Belgium; info@alphabiotoxine.be (R.F.); aude.violette@alphabiotoxine.com (A.V.)
- * Correspondence: bgfry@uq.edu.au; Tel.: +61-7-336-58515



Citation: Dobson, J.S.; Harris, R.J.; Zdenek, C.N.; Huynh, T.; Hodgson, W.C.; Bosmans, F.; Fourmy, R.; Violette, A.; Fry, B.G. The Dragon's Paralysing Spell: Evidence of Sodium and Calcium Ion Channel Binding Neurotoxins in Helodermatid and Varanid Lizard Venoms. *Toxins* **2021**, *13*, 549. <https://doi.org/10.3390/toxins13080549>

Received: 9 July 2021
Accepted: 27 July 2021
Published: 6 August 2021

Publisher's Note: MDPI stays neutral with regard to jurisdictional claims in published maps and institutional affiliations.



Copyright: © 2021 by the authors. Licensee MDPI, Basel, Switzerland. This article is an open access article distributed under the terms and conditions of the Creative Commons Attribution (CC BY) license (<https://creativecommons.org/licenses/by/4.0/>).

Abstract: Bites from helodermatid lizards can cause pain, paresthesia, paralysis, and tachycardia, as well as other symptoms consistent with neurotoxicity. Furthermore, in vitro studies have shown that *Heloderma horridum* venom inhibits ion flux and blocks the electrical stimulation of skeletal muscles. Helodermatids have long been considered the only venomous lizards, but a large body of robust evidence has demonstrated venom to be a basal trait of Anguimorpha. This clade includes varanid lizards, whose bites have been reported to cause anticoagulation, pain, and occasionally paralysis and tachycardia. Despite the evolutionary novelty of these lizard venoms, their neuromuscular targets have yet to be identified, even for the iconic helodermatid lizards. Therefore, to fill this knowledge gap, the venoms of three *Heloderma* species (*H. exasperatum*, *H. horridum* and *H. suspectum*) and two *Varanus* species (*V. salvadorii* and *V. varius*) were investigated using *Gallus gallus* chick biventer cervicis nerve–muscle preparations and biolayer interferometry assays for binding to mammalian ion channels. Incubation with *Heloderma* venoms caused the reduction in nerve-mediated muscle twitches post initial response of avian skeletal muscle tissue preparation assays suggesting voltage-gated sodium (Na_V) channel binding. Congruent with the flaccid paralysis inducing blockage of electrical stimulation in the skeletal muscle preparations, the biolayer interferometry tests with *Heloderma suspectum* venom revealed binding to the S3–S4 loop within voltage-sensing domain IV of the skeletal muscle channel subtype, $\text{Na}_V1.4$. Consistent with tachycardia reported in clinical cases, the venom also bound to voltage-sensing domain IV of the cardiac smooth muscle calcium channel, $\text{Ca}_V1.2$. While *Varanus varius* venom did not have discernable effects in the avian tissue preparation assay at the concentration tested, in the biointerferometry assay both *V. varius* and *V. salvadorii* bound to voltage-sensing domain IV of both $\text{Na}_V1.4$ and $\text{Ca}_V1.2$, similar to *H. suspectum* venom. The ability of varanid venoms to bind to mammalian ion channels but not to the avian tissue preparation suggests prey-selective actions, as did the differential potency within the *Heloderma* venoms for avian versus mammalian pathophysiological targets. This study thus presents the detailed characterization of *Heloderma* venom ion channel neurotoxicity and offers the first evidence of varanid lizard venom neurotoxicity. In addition, the data not only provide information useful to understanding the clinical effects produced by envenomations, but also reveal their utility as physiological probes, and underscore the potential utility of neglected venomous lineages in the drug design and development pipeline.

Keywords: *Heloderma*; *Varanus*; venom; Toxicofera; neurotoxic; sodium channel; calcium channel

Key Contribution: This study identifies modes of action for helodermatid lizard neurotoxins. It also offers the first evidence of neurotoxicity in varanid lizards.

1. Introduction

Voltage-gated ion channels allow the movement of ions across cellular membranes, regulating resting and action potentials. Depending on the type of ions transported, they are categorized as voltage-gated sodium (Na_V), calcium (Ca_V), potassium (K_V), or chloride channels (CLC) [1]. Due to their common evolutionary origin, Na_V , Ca_V and K_V channels share architectural similarities [2]. Their α -subunits are comprised of four identical or homologous domains each, with associated voltage-sensing domains (I–IV). Each domain consists of six transmembrane segments (S1–S6). Segments S5–S6 form the ion-selective pore while S1–S4 form the voltage sensor. In Na_V channels, voltage-sensing domains I–III are important in channel opening while voltage-sensing domain IV is involved in gating regulation and the fast termination of ion flux post-activation [3–5]. Similarly, in Ca_V gating, voltage-sensing domains II and III make a major contribution to channel activation, while voltage-sensing domain I are thought to have a minor role in activation [6]. The potential role of voltage-sensing domain IV in Ca_V fast inactivation is still debated [6,7].

Ion channels are divided into closely related subcategories with specific physiological roles and are often more highly expressed in particular locations within the nervous system. For example, $\text{Na}_V1.4$ and $\text{Na}_V1.5$ are predominantly expressed in skeletal and cardiac muscle, respectively, whereas $\text{Na}_V1.6$ are found in both the CNS and peripheral nervous system (PNS) [8]. Similarly, the L-type Ca_V channels show tissue-selective expression, with $\text{Ca}_V1.1$ abundant in skeletal muscle and $\text{Ca}_V1.2$ in cardiac muscle [1,9]. Both Na_V and Ca_V channels play roles in neurotransmission, endocrine secretion, muscle contraction and sensory perception [10–14]. Therefore, Na_V and Ca_V channels in physiologically relevant locations have been convergently bound by neurotoxins produced by venomous organisms to aid in prey capture and deter potential predators [15].

Ultimately, ion channel-binding toxins can lead to an increase in, or inhibition of, the release of the cholinergic neurotransmitter acetylcholine. Toxins can bind to the pore region or bind to the various voltage-sensing domains, to inhibit ion channel opening, allow opening at more negative voltages, or delay the inactivation of the channel, thus prolonging ion flux [16]. Common targets of ion channel-binding toxins are the extracellular loops between S3 and S4, a region that flexes in response to membrane depolarizations and drives voltage-sensor activation. As the voltage-sensing domains are structurally similar, toxins that interact with this motif often interact with multiple voltage-sensing domains [17]. Toxins that bind to this locus in voltage-sensing domains I–III typically inhibit channel opening, while toxins that exclusively target voltage-sensing domain IV delay fast inactivation, resulting in spastic paralysis, such as that of the elapid snake *Calliophis bivirgatus* [18]. However, exceptions to this paradigm have been found. A toxin isolated from the tarantula *Hysteroocrates gigas* interacts with voltage-sensing domains III and IV to inhibit Ca_V channel gating [19]. Similarly, ProTx-II from the tarantula *Thrixopela pruriens* inhibits Na_V channel gating via voltage-sensing domains II and IV binding [20], which may cause flaccid paralysis.

Despite their evolutionary novelty, lizard venoms are a neglected area of research. From a clinical perspective, members of the *Heloderma* genus are an under-investigated venomous reptile lineage partly due to envenomations rarely requiring medical assistance. Bites with serious symptoms are infrequent, often following a bite where the lizard has been attached to the victim for a considerable amount of time, maximizing venom delivery [21–23]. This is due to their venom apparatus lacking associated muscles the high-pressure venom delivery seen in snakes. Instead, helodermatid lizards possess mandibular

venom glands with multiple ducts leading to the gums at the base of grooved teeth [24]. Therefore, clamping and chewing is required to deliver venom [22].

In addition to coagulotoxic, myotoxic and cytotoxic traits, *Heloderma* bites are often reported to cause pain, paresthesia, tachycardia and paralysis consistent with neurotoxic/cardiotoxic envenomation [23,25,26]. Previous research on *Heloderma* venom has revealed a myriad of protein families often recruited as neurotoxins [24,27–30]. However, few toxins have been isolated and characterized. Injecting purified helothermine, a Cysteine-rich secretory protein (CRiSP) family toxin isolated from *H. horridum*, produces lethargy, rear limb paralysis and death in rodents [31]. Further studies revealed that helothermine selectively binds ryanodine receptors and blocks K^+ and Ca^{2+} ion flux in rat cerebellar cells [32–34]. Komori et al. (1988) reported on the inhibitory effect of “lethal toxin-1” isolated from *H. horridum* on the direct electrical stimulation of mouse hemidiaphragm [35]. This toxin was later revealed to be constructed of β -defensin domain repeats, thus inducing the renaming of the toxin as helofensin [36]. However, the physiological targets of helofensins and helothermine have yet been determined.

Helodermatid lizards were long thought to be the only venomous lizards. However, studies in many “omics” fields have provided evidence for venom in other anguimorph lizard lineages, including varanid species, such as the legendary Komodo dragon (*Varanus komodoensis*) [24,37–41]. The majority of varanid lizards are active predators that exhibit extreme differences in size between species: from the 20 cm *V. sparnus* to the over 2 m *V. komodoensis* [42,43]. This disparity in size is also accompanied by variations in diet, hunting behavior and habitat [43–45]. Differences in selection pressures due to the variety in the habits of these lizards have led to considerable variation in their venom compositions and activities, rivalling that of the diversity seen within genera of venomous snakes, consistent with active evolution under purifying selection pressure [37,38]. Previous studies incubating varanid venoms with human fibrinogen revealed extensive variation in fibrinolytic activity, and other effects include the induction of hypotension [37–40]. Variable venom activity is reflected in the severity of bites in reports, ranging from minor injuries to hospitalizations requiring medical treatment [46–49].

The toxins likely responsible for coagulotoxic activities in varanid lizards are kallikrein enzymes, which destructively cleave fibrinogen, and phospholipase A_2 (PLA $_2$), which block platelet aggregation, with both toxin types being homologous to *Heloderma* toxins with the same activity, reflective of their shared molecular evolutionary history and arising from the same venom glands [37,38,40,50,51]. However, many toxin families often recruited as neurotoxins in other organisms, such as AVIT, PLA $_2$, cysteine rich secretory proteins (CRiSPs) and kunitz peptides, have been identified in the venom gland transcriptomes or venom proteomes of varanid and helodermatid lizards [15,24,27–30,37,40]. Indeed, the neurotoxic peptides in the AVIT and cholecystoxin classes were likely responsible for the strong contraction of rat smooth muscle after incubation with *V. varius* venom [37,38]. In addition, a study noted that injecting birds and rodents with crude *V. griseus* venom resulted in immediate paralysis of rodents, suggesting the presence of taxon-selective receptor-binding neurotoxins [48,52].

Human envenomations by varanid lizards that present with neurotoxic symptoms are rare, but have been reported. Due to the similarities of their venom apparatus to those of *Heloderma*, symptoms of envenomation by varanids follow incidents where the lizard has been attached to the victim for considerable time [46–48]. Whilst bites from larger species such as *V. varius* and *V. salvadorii* have anticoagulant effects, any neurotoxic symptoms caused may be masked by the pain caused by the often severe mechanical damage these species can inflict [49]. However, bites from *V. griseus* have been reported to produce specific symptoms (muscle weakness, local and systemic pain, respiratory distress and difficulty walking), and tests of the venoms on animal models have confirmed these actions [46–48]. The site of action, however, remains enigmatic. Similarly, other victims have observed neurotoxic symptoms post-bites from *V. scalaris*, comparing the sensation to that of a paper wasp sting [44,49].

Despite the evidence presented for neurotoxins within varanid lizard venoms, few studies have investigated the activity of the venom on assays assessing neurotoxicity. Furthermore, studies have yet identified the neurological targets of *Heloderma* venom neurotoxins. Therefore, to fill these knowledge gaps, we investigated the neuropathology of helodermatid and varanid lizard venoms. To observe the effects on whole receptors, we used the *Gallus gallus* chick biventer nerve–muscle preparation assay, an avian skeletal muscle preparation well-validated through numerous studies on snake venoms [18,53–56]. To determine the binding affinity of the venoms for various ion channels, we used biolayer interferometry to ascertain binding to the voltage-sensing domain IV S3–S4 extracellular loop mimotopes for human sodium and calcium channels, an approach validated using venoms as diverse as snakes and stonefish [57–63]. The present study represents the most rigorous investigation of the ion channel neurotoxicity of the *Heloderma* genus, and the first for varanid lizard venoms. Information regarding the fundamental biochemical actions of the venoms may be of use in the evidence-based design of clinical management strategies for envenomed patients. In addition, the results may reveal useful probes of physiological pathways, or reveal novel lead compounds for the drug design and development pipeline.

2. Results

2.1. *Gallus gallus* Chick Biventer Cervicis Nerve–Muscle Assays

Testing on the avian neuromuscular preparation revealed that the muscle twitch response heights were markedly attenuated when *Heloderma* venoms were added (Figure 1). The most potent of the three *Heloderma* venoms was *H. horridum*, which abolished twitches within 60 min (Figure 1A). The venoms of *H. exasperatum* and *H. suspectum* had similar activities, inhibiting twitches by approximately 80% over the time-course of the experiment (Figure 1). There were no significant differences between responses to the agonists acetylcholine (ACh), carbachol (CCh) and potassium chloride (KCl) in the presence or absence of the venoms, with all groups producing responses comparable to the initial contractile response (Figure 1B). Parallel experiments run with *V. varius* venom did not produce notable results at the concentrations tested on this avian tissue preparation (see Supplementary Data).

2.2. Biolayer Interferometry Assays

As it is a well-described ion channel-attacking venom, *L. quinquestratus* was used as a positive control to validate the assay parameters, displaying strong binding to the S3–S4 extracellular loop mimotope of voltage-sensing domain IV of human Na_v1.4 and Ca_v1.2 (Figure 2A,B and Figure 3A,B, respectively). Wavelength response shifts indicate *Heloderma suspectum* venom binds strongly to the voltage-sensing domain IV motif of human Na_v1.4 (Figure 3A,B) and Ca_v1.2 (Figure 3A,B). In contrast, the other helodermatid lizard species tested, *H. exasperatum* and *H. horridum*, did not display significant binding to these mammalian targets (Figures 2 and 3). However, wavelength response shifts indicate that *V. salvadorii* venom strongly binds to the voltage-sensing domain IV motif of both Na_v1.4 (Figure 2C,D) and Ca_v1.2 (Figure 3C,D). Although still binding significantly, *V. varius* venom was less potent than *V. salvadorii* on both targets, and proportionally weaker on Ca_v1.2 than Na_v1.4 (Figure 2C,D), being equipotent to *H. suspectum* on Ca_v1.2 (Figure 3) but slightly less potent than *H. suspectum* on Na_v1.4 (Figure 2).

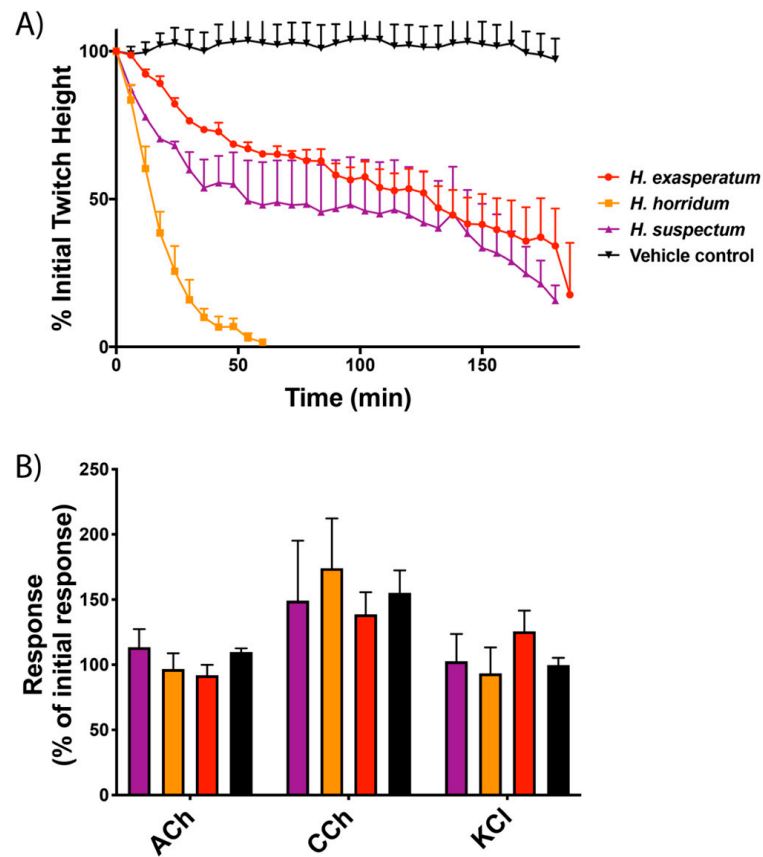


Figure 1. *Gallus gallus* chick biventer cervicis nerve–muscle preparation results after incubation with *Heloderma* venoms; (A) inhibition of indirect muscle twitches by *Heloderma exasperatum* (red), *H. horridum* (orange) and *H. suspectum* (purple) venoms relative to the initial twitches recorded prior to venom addition. Vehicle control shown in black; (B) effect of venoms on the contractile responses of the agonists acetylcholine (ACh), carbachol (CCh) and potassium chloride (KCl) relative to the initial response. All experiments were performed in triplicate.

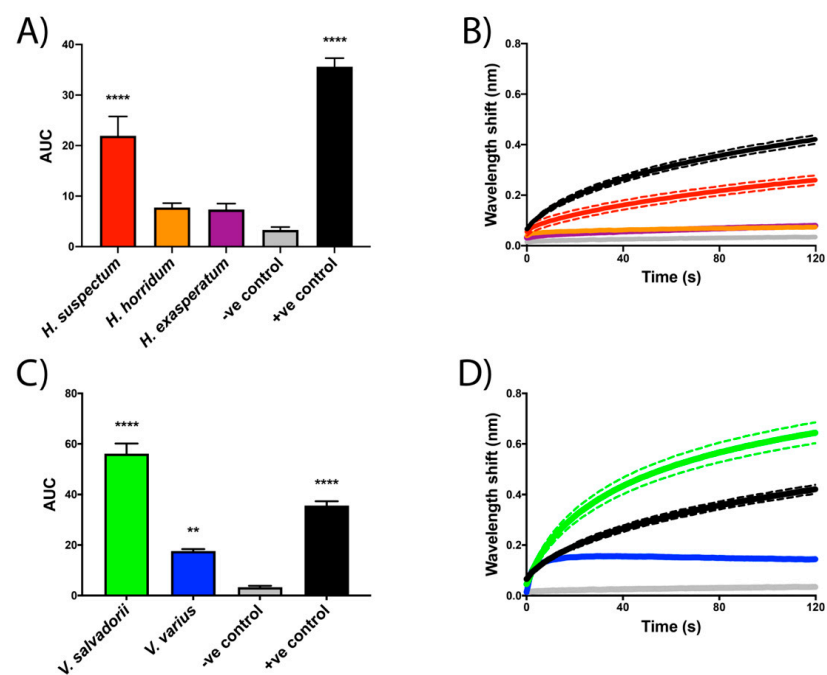


Figure 2. Binding affinity of *Heloderma* (A,B) and *Varanus* (C,D) crude venoms to the S3–S4 extracellular

loop mimotope of domain IV of the human sodium channel Nav1.4. Figures (A,C) depict the area under the curve (AUC) of the curves displayed in figures (B,D). The Y axis of figure (B) shows the wavelength (nm) from the association (Ka binding) step. Asterisk symbols (*) above the bars (A,C) denote the level of statistical significance relative to the negative control. The negative control (-ve) was *Naja kaouthia* crude venom, while the positive control was *Leiurus quinquestriatus* crude venom. Dotted lines surrounding curves represent the error bars (B,D) based on SEM values from experiments performed in triplicate.

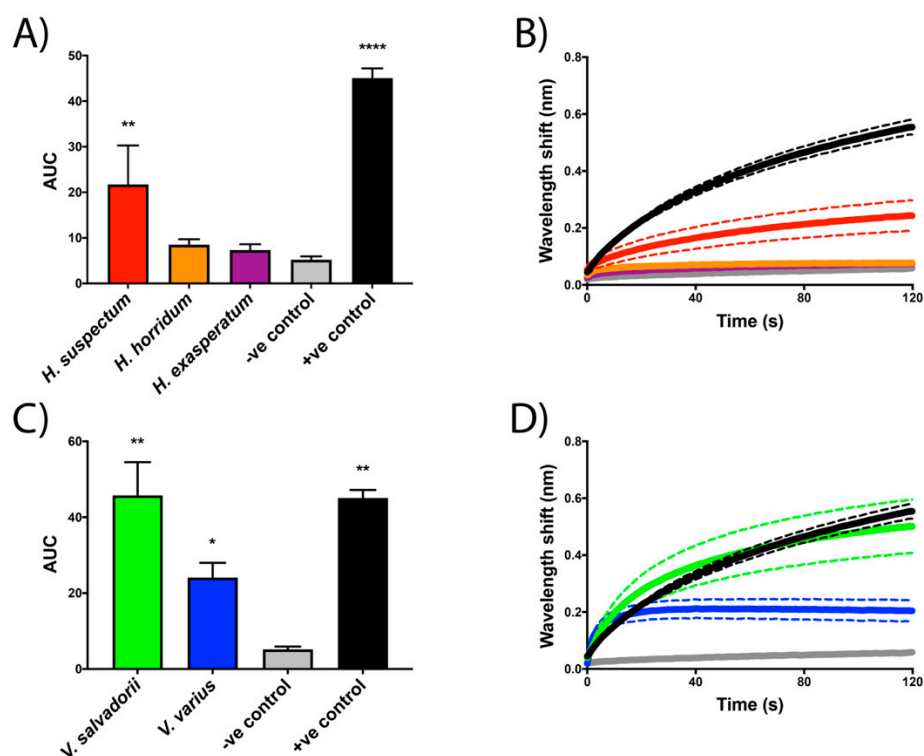


Figure 3. Binding affinity of *Heloderma* (A,B) and *Varanus* (C,D) crude venoms to the S3–S4 extracellular loop mimotope of domain IV of the human calcium channel Cav1.2. Figures (A,C) depict the area under the curve (AUC) of the curves displayed in (B,D). The Y axis of (B) shows the wavelength (nm) from the association (Ka binding) step. Asterisk symbols (*) above the bars (B,D) denote the level of statistical significance relative to the negative control. The negative control (-ve) was *Naja kaouthia* crude venom while the positive control was *Leiurus quinquestriatus* crude venom. Dotted lines surrounding curves (C,D) represent the error bars based on SEM values from experiments performed in triplicate.

3. Discussion

Helodermatid lizard venoms have previously been shown to inhibit the electrical stimulation of mouse hemidiaphragm and induce paralysis in mice [31,35], but the site of action was not determined in this prior work. Here, we present similar results displaying a reduction in contraction ability in avian skeletal muscle (Figure 1A). Responses to postsynaptic agonists suggest *Heloderma* venoms act pre-synaptically, with the absence of myotoxicity (Figure 1B). Congruent with the avian tissue preparation results of presynaptic neurotoxicity, bilayer interferometry assays revealed *Heloderma suspectum* bound to the S3–S4 loop of voltage-sensing domain IV within Nav1.4, inhibiting channel fast inactivation and altering Na⁺ influx (Figure 2A,B). While many toxins that bind to voltage-sensing domain IV have a stimulatory effect, such as delaying inactivation [18], binding to produce an inhibitory effect has been documented [20], thus supporting our results. In addition, many toxins found to bind to voltage-sensing domain IV also interact with voltage sensing domains I–III, where binding would inhibit gating [17]. The dichotomy between the avian

tissue preparation and the mammalian-target biolayer interferometry assays is suggestive of differential taxon-specific effects between the three *Heloderma* species tested and thus is a rich area for future research regarding the evolutionary selection pressures leading to such lineage-selective effects.

While *V. varius* venom did not produce discernable results on the avian-tissue preparation assays at the concentrations tested, both *V. varius* and *V. salvadorii* bound mammalian Na_v1.4 with *V. varius* nearly equipotent to *H. suspectum* while *V. salvadorii* was almost twice as potent (Figure 2). These results support the clinical symptoms of lethargy and paralysis reported in the bites from helodermatid and, occasionally, varanid lizards [21,46,48]. Further support can be found from previously conducted in vivo studies [31,35,52]. *Varanus griseus* venom is reported to produce paralyzing effects on mice, consistent with Na_v1.4 antagonistic activity, similar to the effects of helothermine [31,52]. The study by Gorelov (1971) also injected sparrows with *V. griseus* venom, which did not result in the immediate paralysis observed in mice, corroborating the lack of effect of the varanid venoms on the avian tissue preparation assays and the strong binding in mammalian target assays.

The disparity between avian and mammalian data is suggestive of differences in ion channel physiology between organisms. Structural differences between voltage-gated ion channels of avian and mammalian species (as shown in the sequence variation of key domains in uniprot accessions P35499 and P35499) could explain the lack of venom activity displayed by the varanid lizards in avian tissue preparation assays and the strong binding in mammalian biolayer interferometry assays, and the converse where *H. exasperatum* and *H. horrium* were much more potent in the avian assay than the mammalian (Figures 1–3). As the *Heloderma* and *Varanus* species studied here are known to consume both mammals and birds, different toxin classes may be selected for the subjugation of different prey, as has been observed for snake venoms [64]. Such differences observed for snake venoms include extreme variations between prey lineages, suggestive of taxon-specific effects [65–71]. Other lineage-specific effects include the binding affinity of μ -conotoxins, which are significantly more potent binders of frog TTX-resistant Na_v channels as compared to homologous channels in rat and mouse assays and while such variation is not reflective of any sort of biological reality (as cone snails do not feed on frogs or rodents) this specificity of venoms never-the-less underscores the potential use of venoms as probes for differences in physiological pathways of disparate animal lineages [72,73].

Compared to other *Heloderma* venoms tested, *H. horridum* venom was more potent on avian tissue preparation assays (Figure 1) and showed a lower binding affinity to the mammalian ion channel domains, possibly reflecting a predatory role of the venom with variations in diet between *Heloderma* species. Due to the elusive subterranean nature of *Heloderma* species, studies on diet comparisons are lacking, often limited to seasonal above-ground observations. Thus, the abundant observations of helodermatid lizard diets preying upon defenseless prey, such as eggs and nestlings [25,43,74], are likely due to the opportunistic nature of these observations when the lizards are feeding upon birds and eggs during annual avian breeding periods. Supporting this supposition are records of *H. suspectum* consuming mammals, which rapidly succumb to the venom's effects ([75], Fry's personal observations).

An alternative testable hypothesis is that differences in venom activity between species could be selected for defensive purposes. *Heloderma suspectum* are the smaller of the species tested and thus are likely more vulnerable to mammalian predators, such as *Canis latrans* [25]. This is consistent with the more prominent aposematic markings found on *H. suspectum*, indicating that a bite causes pain. Indeed, severe pain is often recorded in bite reports from this species [76]. Many varanid lizard species are also vulnerable to mammalian and avian predators as juveniles, and for smaller species, as adults; therefore, a painful bite would confer an advantage [43]. It is unclear if the activity presented in this study may contribute to the pain from a bite, as there is extensive cross-reactivity between sodium channel types, and thus paralytic toxins binding to the neuromuscular target Na_v1.4 may also bind to other sodium channels involved in pain. However, the

interactions of $\text{Na}_V1.4$ shown in this study would produce paralysis of skeletal muscles, such as is shown in the tissue preparation, which is consistent with evolutionary selection pressures for a predatory role. Thus, a testable hypothesis for future work is that *Heloderma* venom contains components for prey subjugation, in addition to serving a defensive role due to the cross-reactivity between sodium channel subtypes.

Commonly reported in severe *Heloderma* human bite clinical cases are tachycardia, arrhythmia, and the potentially fatal cardiac ischemia [22,23,76]. An increased, irregular heart rate has also been observed following varanid lizard bites [46,48]. As $\text{Ca}_V1.2$ is primarily a cardiac muscle ion channel, binding to this channel could be the mode of action responsible for these symptoms. Harris et al. (2021) reported on the binding of stone fish (*Synanceia verrucosa*) venom to the S3–S4 extracellular loop of voltage-sensing domain IV of $\text{Ca}_V1.2$, suggesting this activity could explain the arrhythmia and tachycardia that manifest post-stone fish envenomation. In addition, severe scorpion envenomations can cause cardiac ischemia [77]. A direct cardiac effect may act synergistically with the mass release of catecholamines that has been suggested as the cause of similar symptoms seen in *Heloderma* bite victims [76]. Thus, the role of the $\text{Ca}_V1.2$ binding effect is another rich area for future research into the predatory or defensive ecology of anguimorph lizard. In addition to the calcium channel-binding toxins, the effects upon heart rate may also be due to the sodium channel-binding toxins binding to the cardiac-associated $\text{Na}_V1.5$ channel [8]. While not investigated in this study, toxins that bind to $\text{Na}_V1.4$ have also been reported to bind to other Na_V channels, including $\text{Na}_V1.5$ [78]. Thus, the ion channel interactions responsible for cardiac dysfunction is another rich area of future research.

Venom binding to both Na_V and Ca_V channels is often due to the possession of a complex cocktails of toxins which individually may have selective binding affinities for either channel family. Conversely, some toxins are promiscuous in being able to bind across not only Na_V or Ca_V channel subtypes, but due to the homologous architecture from a shared molecular evolutionary history, some ion channel toxins are able to act upon both Na_V and Ca_V channels. Examples include hanatoxin, which binds to multiple subtypes of Na_V , Ca_V and K_V channels [16]. Similarly, other tarantula venom peptides have been found to be active on both Na_V and Ca_V channels [79]. Thus, the structure-function responsible for such diverse binding by some venom toxins is a rich area for future research.

Based on the results presented in this study, future work should investigate other species of varanid lizards for their potential neurotoxic venom activities. While we were limited by species available, experiments should be performed on species previously shown to produce neurotoxic activities and symptoms, such as *V. griseus*, *V. scalaris*, and other closely related species. Binding to the S3–S4 extracellular loop of domains I–III could potentially be investigated using bilayer interferometry mimotope assays similar to those used in this study. Despite evidence of toxins binding to the voltage-sensing domain IV of $\text{Na}_V1.4$ and $\text{Ca}_V1.2$, translating these data into the effects on whole ion channel gating would require future work on additional testing platforms, such as the K_V channel chimeric approach or electrophysiological techniques such as oocyte patch-clamp assays. In addition, future work should include fractionating the venoms to ascertain the toxin types responsible for these intriguing activities.

In summary, we have elucidated the calcium and sodium channel-binding mechanisms of *Heloderma* venom, and report for the first time evidence of ion channel binding neurotoxins in *Varanus* venoms. This work provides a foundation for natural history investigations to ascertain the biological roles of lizard venoms, whether as predatory weapons or as part of a defensive arsenal, or a combination thereof. Notably, the neurotoxic effects revealed in this study are indicative of both defensive and predatory roles for the venoms of *Heloderma* and *Varanus* species, and further suggest prey-selective effects of both *Heloderma* and *Varanus* venoms. The modes of action of these venoms presented in this study could also be important in understanding the clinical effects of envenomations, by revealing the underlying biochemistry of neurotoxic symptoms, thereby providing data which may be useful for the evidence-based design of clinical management strategies. The

results further underscore the utility of using venoms as rich sources of novel compounds, useful as probes to ascertain physiological function, and even as lead compounds for drug design and development. Animal toxins have been used as key probes in the discovery of voltage-gated ion channel subtypes, their structural properties, and their functional characteristics. Our results reinforce the use of bilayer interferometry assays as a potential tool to investigate the role of voltage-sensing domains in ion channel gating. Thus, in addition to being selective probes for ion channel functions, these novel compounds may have utility as starting substrates in the drug design and development pipeline. It is only by investigating the full range of venomous animals, such as the neglected venomous lizard lineages, that such resources can be harnessed to their fullest potential.

4. Materials and Methods

4.1. Sample Acquisition

Venoms were collected by encouraging the specimens to chew on soft rubber tubing, with the mandibular secretions collected with pipettes (*Varanus*) or allowed to flow into a 50 mL tube (*Heloderma*). Secretions were then centrifuged at 14,000 RCF (4 °C, 10 min.) to remove insoluble material, filtered with a 40 µm syringe filter, flash-frozen in liquid nitrogen, and then freeze-dried. *Varanus varius* samples (adult male, $n = 3$, pooled) were collected from captive specimens under University of Queensland animal ethics approval SBS/403/16 (approval date: 1 February 2016). Non-Australian lizard (*H. exasperatum*, *H. horridum*, *H. suspectum*, and *V. salvadorii*) samples were supplied by licensed biotechnology company Alphabiotoxine Laboratory, Montroel-au-bois, Belgium.

4.2. Gallus Gallus Chick Biventer Cervicis Nerve–Muscle Assays

Neurotoxicity was ascertained using a previously validated organ bath protocol [80]. *Gallus gallus* chicks aged between 4–10 days were euthanized with CO₂ (animal ethics number 22575 was approved by Monash University Ethics Committee on 18 December 2019). Biventer cervicis nerve–muscle samples were removed and mounted under 1 g tension in 5 mL organ baths containing physiological salt solution (NaCl, 118.4 mM; KCl, 4.7 mM; MgSO₄, 1.2 mM; KH₂PO₄, 1.2 mM; CaCl₂, 2.5 mM; NaHCO₃, 25 mM; and glucose, 11.1 mM). Organ baths were bubbled with carbogen (95% O₂; 5% CO₂) at a constant temperature of 34 °C. Electrodes were placed around the tendon of the biventer muscle and electrical stimulation at the motor nerve (0.2 ms duration, 0.1 Hz, supramaximal V) using a Grass S88 stimulator (Grass Instruments, Quincy, MA, USA) evoked indirect twitches. Selective stimulation of the nerve was confirmed by the abolition of twitches with d-tubocurarine (10 µM), a nAChR competitive antagonist. Tissues were then washed repeatedly with physiological salt solution to restore twitch responses to nerve stimulation. The stimulation was ceased, and the contractile responses to acetylcholine (ACh, 1 mM for 30 s), carbochol (CCh, 20 µM for 60 s), and potassium chloride (KCl, 40 mM for 30 s) were obtained and recorded. The organ bath was then washed, and electrical stimulation was resumed and maintained for 30 min to allow the preparation to equilibrate. Venom (10 µg/mL) was added to the organ bath, and the twitch height was recorded until the abolition of twitch response or was stopped after a 1 h period. The stimulator was turned off again and the bath was washed. Contractile responses to ACh, CCh and KCl were obtained again to compare with responses prior to venom addition. The twitch responses to electrical stimulation and contractile responses to agonists (ACh, CCh, and KCl) were measured using a Grass FT03 force displacement transducer (Grass Instruments, Quincy, MA, USA) and recorded on a PowerLab system (ADInstruments Pty Ltd., Bella Vista, NSW, Australia). The data were then converted into figures using Prism8.0 software (GraphPad Software Inc., La Jolla, CA, USA).

4.3. Bilayer Interferometry

The voltage-sensing domain IV S3–S4 motifs were ascertained using previously validated protocols [57,81]. The amino acid sequences for human voltage-sensing domain IV S3–S4 motifs are shown in Figure 4 for Ca_v1.2 (Homo sapiens, uniprot accession code

Q13936) and Nav1.4 (Homo sapiens, uniprot accession code P35499). These regions were synthesized by GenicBio Ltd. (Shanghai, China) and joined to two aminohexanoic acid (Ahx) spacers forming a 30 Å linker, with the end Ahx then bound to biotin, providing clearance between the biotin and mimotope and thereby allowing the mimotope to maintain its natural conformational freedom when binding to the analyte in solution. Dried stocks of mimotopes were solubilized in 100% dimethyl sulfoxide (DMSO) prior to dilution with deionized water in a 1:10 ratio to produce a working stock concentration of 50 µg/mL. This stock was then stored at −80 °C until required for experiments. Binding kinetics were analyzed by biolayer interferometry utilizing the Octet HTX system (ForteBio). All assays were conducted in standard Greiner black 96-microtiter well plates (ref: 655209). Analyte (venom) experimental concentrations of 50 µg/mL (10 µg per well) were produced by diluting stock solutions 1:20 with matrix buffer (1× DPBS with 0.1% BSA and 0.05% Tween-20). Mimotope aliquots were diluted 1:50 with matrix buffer to produce a final concentration of 1 µg/mL (0.2 µg per well). Streptavidin sensors were hydrated in the matrix buffer for 30–60 min, whilst being agitated at 2.0 RPM on a shaker prior to experiments. A standard acidic solution glycine buffer (10 mM glycine (pH 1.5–1.7)) in deionized water was used to regenerate the sensor tips during experimentation while still leaving the mimotope attached to the sensor. Controls consisted of a buffer control (deionized water:glycerol 1:1) and the negative control *Naja kaouthia* (monocled cobra) venom in the place of the analyte sample in the wells. The positive control for Nav1.4- and Cav1.2-binding was *Leiurus quinquestriatus* (deathstalker scorpion) venom, which is known to strongly bind to both channels.

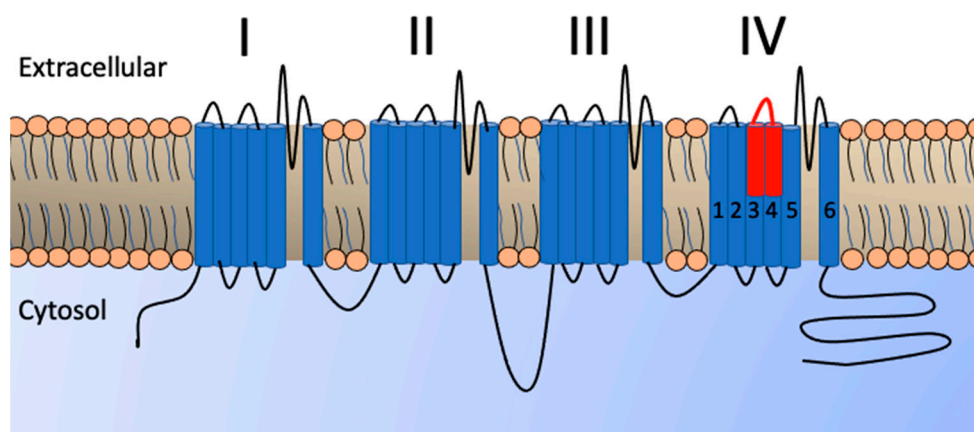


Figure 4. Graphic depicting the basic structure of a voltage-gated ion channel α -subunit displaying the position of the voltage-sensing domains I–IV in the phospholipid bilayer. Blue cylinders represent transmembrane helices while black lines represent connective loops. Highlighted in red is the S3–S4 extracellular loop of voltage-sensing domain IV used in the biolayer interferometry assays. As previously validated [57,80], biosensor mimotopes were designed from sequences for this region, as follows: for Cav1.2 (Homo sapiens), AEHTQSSPSMNAEENSRSISITFFRLFRVMRLVK, and for Nav1.4 (Homo sapiens), SIVGLALSDLIQKYFVSPTLFRVIRLARIGRVLRL.

Data were processed in accordance with the validation study [59]. The association step data (.csv file) were extracted for each triplicate and imported into Prism 9.0 software (GraphPad Software Inc., La Jolla, CA, USA) where area under the curve (AUC) calculations were made and data graphed. Dunnett’s multiple comparison tests were performed to determine statistical significances between treatment groups and negative controls.

Supplementary Materials: The following are available online at <https://www.mdpi.com/article/10.3390/toxins13080549/s1>, S1: Raw Data.

Author Contributions: Conceptualization, B.G.F. and F.B.; methodology, F.B. and W.C.H.; validation, R.J.H., C.N.Z., T.H. and W.C.H.; formal analysis, J.S.D.; writing—original draft preparation, J.S.D.; writing—review and editing, R.J.H., C.N.Z., T.H., W.C.H., F.B., R.F., A.V. and B.G.F. Sample provision, B.G.F., R.F. and A.V. All authors have read and agreed to the published version of the manuscript.

Funding: This research was funded by Australian Research Council Discovery Project DP210102406 and Australian Research Council Linkage Infrastructure & Equipment Fund LE200100140 to BGF. T.H. and W.C.H. were supported by an Australian National Health and Medical Research Council (NHMRC) Centres for Research Excellence Grant (ID: 1110343).

Institutional Review Board Statement: *Varanus varius* samples (adult male, $n = 3$, pooled) were collected from captive specimens under University of Queensland animal ethics approval SBS/403/16 (approval date: 1 February 2016). Non-Australian lizard (*H. exasperatum*, *H. horridum*, *H. suspectum*, and *V. salvadorii*) samples were supplied by licensed biotechnology company Alphabiotoxine Laboratory, Montroel-au-bois, Belgium.

Informed Consent Statement: Not applicable.

Data Availability Statement: The data presented in this study are available in supplementary material.

Conflicts of Interest: The authors declare no conflict of interest.

References

1. Ertel, E.A.; Campbell, K.P.; Harpold, M.M.; Hofmann, F.; Mori, Y.; Perez-reyes, E.; Schwartz, A.; Snutch, T.P.; Tanabe, T.; Birnbaumer, L.; et al. Nomenclature of Voltage-Gated Calcium Channels. *Neuron* **2000**, *25*, 533–535. [\[CrossRef\]](#)
2. Anderson, P.A.V.; Greenberg, R.M. Phylogeny of Ion Channels: Clues to Structure and Function. *Comp. Biochem. Physiol. Part B* **2001**, *129*, 17–28. [\[CrossRef\]](#)
3. Ahern, C.A.; Payandeh, J.; Bosmans, F.; Chanda, B. The Hitchhiker’s Guide to the Voltage-Gated Sodium Channel Galaxy. *J. Gen. Physiol.* **2016**, *147*, 1–24. [\[CrossRef\]](#)
4. Chanda, B.; Bezanilla, F. Tracking Voltage-Dependent Conformational Changes in Skeletal Muscle Sodium Channel during Activation. *J. Gen. Physiol.* **2002**, *120*, 629–645. [\[CrossRef\]](#) [\[PubMed\]](#)
5. Goldschen-ohm, M.P.; Capes, D.L.; Oelstrom, K.M.; Chanda, B. Multiple Pore Conformations Driven by Asynchronous Movements of Voltage Sensors in a Eukaryotic Sodium Channel. *Nat. Commun.* **2013**, *4*, 1350. [\[CrossRef\]](#) [\[PubMed\]](#)
6. Pantazis, A.; Savalli, N.; Sigg, D.; Neely, A.; Olcese, R.; Pantazisa, A.; Savalli, N.; Sigg, D.; Neely, A.; Olcese, R. Functional Heterogeneity of the Four Voltage Sensors of a Human L-type Calcium Channel. *Proc. Natl. Acad. Sci. USA* **2021**, *111*, 18381–18386. [\[CrossRef\]](#) [\[PubMed\]](#)
7. Beyl, S.; Depil, K.; Hohaus, A.; Stary-weinzinger, A.; Linder, T.; Timin, E.; Hering, S. Neutralisation of a Single Voltage Sensor Affects Gating Determinants in All Four Pore-Forming S6 Segments of CaV1.2: A Cooperative Gating Model. *Pflügers Arch.-Eur. J. Physiol.* **2012**, *464*, 391–401. [\[CrossRef\]](#) [\[PubMed\]](#)
8. Catterall, W.A.; Goldin, A.L.; Waxman, S.G. International Union of Pharmacology. XLVII. Nomenclature and Structure-Function Relationships of Voltage-Gated Sodium Channels. *Pharmacol. Rev.* **2005**, *57*, 397–409. [\[CrossRef\]](#)
9. Dolphin, A.C. Calcium Channel Diversity: Multiple Roles of Calcium Channel Subunits. *Curr. Opin. Neurobiol.* **2009**, *19*, 237–244. [\[CrossRef\]](#)
10. Catterall, W.A. Voltage-Gated Calcium Channels. *Cold Spring Harb. Perspect. Biol.* **2011**, *3*, 1–23. [\[CrossRef\]](#)
11. Catterall, W.A. Voltage-Gated Sodium Channels at 60: Structure, Function and Pathophysiology. *J. Physiol.* **2012**, *590*, 2577–2589. [\[CrossRef\]](#)
12. George, A.L.J. Inherited Disorders of Voltage-Gated Sodium Channels. *J. Clin. Investig.* **2005**, *115*, 1990–1999. [\[CrossRef\]](#) [\[PubMed\]](#)
13. Cannon, S.C. Pathomechanisms in Channelopathies of Skeletal Muscle and Brain. *Annu. Rev. Neurosci.* **2006**, *29*, 387–417. [\[CrossRef\]](#) [\[PubMed\]](#)
14. Waxman, S.G.; Merckies, I.S.J.; Gerrits, M.M.; Dib-hajj, S.D.; Lauria, G.; Cox, J.J.; Wood, J.N.; Woods, C.G.; Drenth, J.P.H.; Faber, C.G. Sodium Channel Genes in Pain-Related Disorders: Phenotype–Genotype Associations and Recommendations for Clinical Use. *Lancet Neurol.* **2014**, *13*, 1152–1160. [\[CrossRef\]](#)
15. Fry, B.G.; Roelants, K.; Champagne, D.E.; Scheib, H.; Tyndall, J.D.A.; King, G.F.; Nevalainen, T.J.; Norman, J.A.; Lewis, R.J.; Norton, R.S.; et al. The Toxicogenomic Multiverse: Convergent Recruitment of Proteins Into Animal Venoms. *Annu. Rev. Genomics Hum. Genet.* **2009**, *10*, 483–511. [\[CrossRef\]](#) [\[PubMed\]](#)
16. Bosmans, F.; Swartz, K.J. Targeting Voltage Sensors in Sodium Channels with Spider Toxins. *Trends Pharmacol. Sci.* **2010**, *31*, 175–182. [\[CrossRef\]](#) [\[PubMed\]](#)
17. Bosmans, F.; Martin-Eauclaire, M.F.; Swartz, K.J. Deconstructing Voltage Sensor Function and Pharmacology in Sodium Channels. *Nature* **2008**, *456*, 202–208. [\[CrossRef\]](#)

18. Yang, D.C.; Deuis, J.R.; Dashevsky, D.; Dobson, J.; Jackson, T.N.W.; Brust, A.; Xie, B.; Koludarov, I.; Debono, J.; Hendrikx, I.; et al. The Snake with the Scorpion's Sting: Novel Three-Finger Toxin Sodium Channel Activators from the Venom of the Long-Glanded Blue Coral Snake (*Calliophis bivirgatus*). *Toxins* **2016**, *8*, 303. [[CrossRef](#)]
19. Bourinet, E.; Stotz, S.C.; Spaetgens, R.L.; Dayanithi, G.; Lemos, J.; Nargeot, J.; Zamponi, G.W. Interaction of SNX482 with Domains III and IV Inhibits Activation Gating of $\alpha 1E$ (CaV2.3) calcium channels. *Biophys. J.* **2001**, *81*, 79–88. [[CrossRef](#)]
20. Gilchrist, J.; Bosmans, F. Using Voltage-Sensor Toxins and their Molecular Targets to Investigate NaV1.8 Gating. *J. Physiol.* **2018**, *10*, 1863–1872. [[CrossRef](#)]
21. Hooker, K.R.; Caravati, M.E. Gila Monster Envenomation. *Ann. Emerg. Med.* **1994**, *24*, 731–735. [[CrossRef](#)]
22. French, R.N.E.; Ash, J.; Brooks, D.E.; French, R.N.E.; Ash, J.; Brooks, D.E. Gila Monster Bite. *Clin. Toxicol.* **2012**, *50*, 151–152. [[CrossRef](#)] [[PubMed](#)]
23. Amri, K.; Chippaux, J. Report of a Severe *Heloderma suspectum* Envenomation. *Clin. Toxicol.* **2020**, *59*, 343–346. [[CrossRef](#)]
24. Fry, B.G.; Winter, K.; Norman, J.A.; Roelants, K.; Nabuurs, R.J.A.; van Osch, M.J.P.; Teeuwisse, W.M.; van der Weerd, L.; Mcnaughtan, J.E.; Kwok, H.F.; et al. Functional and Structural Diversification of the Anguimorpha Lizard Venom System. *Mol. Cell. Proteom.* **2010**, *9*, 2369–2390. [[CrossRef](#)]
25. Russell, F.E.; Bogert, C.M. Gila Monster: Its Biology, Venom and Bite—A Review. *Toxicon* **1981**, *19*, 341–359. [[CrossRef](#)]
26. French, R.; Brooks, D.; Ruha, A.; Shirazi, F.; Boesen, K.; Walter, F.; French, R.; Brooks, D.; Ruha, A.; Shirazi, F.; et al. Gila Monster (*Heloderma suspectum*) Envenomation: Descriptive Analysis of Calls to United States Poison Centers with Focus on Arizona Cases. *Clin. Toxicol.* **2015**, *53*, 60–70. [[CrossRef](#)] [[PubMed](#)]
27. Lino-López, G.J.; Valdez-Velázquez, L.L.; Corzo, G.; Romero-Gutiérrez, M.T.; Jiménez-Vargas, J.M.; Rodríguez-Vázquez, A.; Vázquez-Vuelvas, O.F.; Gonzalez-Carrillo, G. Venom Gland Transcriptome from *Heloderma horridum horridum* by High-Throughput Sequencing. *Toxicon* **2020**, *180*, 62–78. [[CrossRef](#)]
28. Koludarov, I.; Jackson, T.N.W.; Sunagar, K.; Nouwens, A.; Hendrikx, I.; Fry, B.G. Fossilized Venom: The Unusually Conserved Venom Profiles of *Heloderma* Species (Beaded Lizards and Gila Monsters). *Toxins* **2014**, *6*, 3582–3595. [[CrossRef](#)] [[PubMed](#)]
29. Kwok, H.F.; Ivanyi, C.; Morris, A.; Shaw, C. Proteomic and Genomic Studies on Lizard Venoms in the Last Decade. *Proteom. Insights* **2010**, *3*, 25–31. [[CrossRef](#)]
30. Sanggaard, K.W.; Dyrland, T.F.; Thomsen, L.R.; Nielsen, T.A.; Brøndum, L.; Wang, T.; Thøgersen, I.B.; Enghild, J.J. Characterization of the Gila Monster (*Heloderma suspectum suspectum*) Venom Proteome. *J. Proteom.* **2015**, *117*, 1–11. [[CrossRef](#)] [[PubMed](#)]
31. Mochca-Morales, J.; Martin, B.M.; Possani, L.D. Isolation and Characterization of Helothermine, a Novel Txin from *Heloderma horridum horridum* (Mexican Beaded Lizard) Venom. *Toxicon* **1990**, *28*, 299–309. [[CrossRef](#)]
32. Morrisette, J.; Krätzschar, J.; Haendler, B.; El-Hayek, R.; Mochca-Morales, J.; Martin, B.M.; Patel, J.R.; Moss, R.L.; Schleuning, W.D.; Coronado, R.; et al. Primary Structure and Properties of Helothermine, a Peptide Toxin that Blocks Ryanodine Receptors. *Biophys. J.* **1995**, *68*, 2280–2288. [[CrossRef](#)]
33. Nobile, M.; Magnelli, V.; Lagostena, L.; Mochca-Morales, J.; Possani, L.D.; Prestipino, G. The Toxin Helothermine Affects Potassium Currents in Newborn Rat Cerebellar Granule Cells. *J. Membr. Biol.* **1994**, *139*, 49–55. [[CrossRef](#)]
34. Nobile, M.; Noceti, F.; Prestipino, G.; Possani, L.D. Helothermine, a Lizard Venom Toxin, Inhibits Calcium Current in Cerebellar Granules. *Exp. Brain Res.* **1996**, *110*, 15–20. [[CrossRef](#)]
35. Komori, Y.; Nikai, T.; Sugihara, H. Purification and Characterization of a Lethal Toxin from the Venom of *Heloderma horridum horridum*. *Biochem. Biophys. Res. Commun.* **1988**, *154*, 613–619. [[CrossRef](#)]
36. Fry, B.G.; Roelants, K.; Winter, K.; Hodgson, W.C.; Griesman, L.; Kwok, H.F.; Scanlon, D.; Karas, J.; Shaw, C.; Wong, L.; et al. Novel Venom Proteins Produced by Differential Domain-Expression Strategies in Beaded Lizards and Gila Monsters (Genus *Heloderma*). *Mol. Biol. Evol.* **2010**, *27*, 395–407. [[CrossRef](#)] [[PubMed](#)]
37. Koludarov, I.; Jackson, T.N.W.; op den Brouw, B.; Dobson, J.; Dashevsky, D.; Arbuckle, K.; Clemente, C.J.; Stockdale, E.J.; Cochran, C.; Debono, J.; et al. Enter the Dragon: The Dynamic and Multifunctional Evolution of Anguimorpha Lizard Venoms. *Toxins* **2017**, *9*, 242. [[CrossRef](#)]
38. Dobson, J.S.; Zdenek, C.N.; Hay, C.; Violette, A.; Fourmy, R.; Cochran, C.; Fry, B.G. Varanid Lizard Venoms Disrupt the Clotting Ability of Human Fibrinogen through Destructive Cleavage. *Toxins* **2019**, *11*, 255. [[CrossRef](#)]
39. Fry, B.G.; Wroe, S.; Teeuwisse, W.; Van Osch, M.J.P.; Moreno, K.; Ingle, J.; Mchenry, C.; Ferrara, T.; Clausen, P.; Scheib, H.; et al. A Central Role for Venom in Predation by *Varanus komodoensis* (Komodo Dragon) and the Extinct Giant *Varanus* (*Megalania*) *priscus*. *Proc. Natl. Acad. Sci. USA* **2009**, *106*, 8969–8974. [[CrossRef](#)]
40. Fry, B.G.; Vidal, N.; Norman, J.A.; Vonk, F.J.; Scheib, H.; Ramjan, S.F.R.; Kuruppu, S.; Fung, K.; Hedges, S.B.; Richardson, M.K.; et al. Early Evolution of the Venom System in Lizards and Snakes. *Nature* **2006**, *439*, 584–588. [[CrossRef](#)] [[PubMed](#)]
41. Koludarov, I.; Sunagar, K.; Undheim, E.A.B.; Jackson, T.N.W.; Ruder, T.; Whitehead, D.; Saucedo, A.C.; Mora, G.R.; Alagon, A.C.; King, G.; et al. Structural and Molecular Diversification of the Anguimorpha Lizard Mandibular Venom Gland System in the Arboreal Species *Abronia graminea*. *J. Mol. Evol.* **2012**, *75*, 168–183. [[CrossRef](#)] [[PubMed](#)]
42. Wilson, S.; Swan, G. *A Complete Guide to Reptiles of Australia*, 5th ed.; Reed New Holland Publishers: Chatswood, Australia, 2017; ISBN 9781925546026.
43. Pianka, E.R.; King, D.; King, R. *Varanoid Lizards of the World*; Pianka, E.R., King, D.R., King, R.A., Eds.; Indiana University Press: Indianapolis, IN, USA, 2004.

44. Pianka, E.R.; Sweet, S.S. Field Observations by Two American Varanophiles. In *Proceedings of the 2015 Interdisciplinary World Conference on Monitor Lizards*; Cota, M., Ed.; Institute for Research and Development, Suan Sunandha Rajabhat University: Bangkok, Thailand, 2016; pp. 1–68.
45. Arbuckle, K. Ecological Function of Venom in *Varanus*, with a Compilation of Dietary Records from the Literature. *Biawak* **2009**, *3*, 46–56.
46. Sopiev, O.; Makeev, V.M.; Kudryavcev, S.V.; Makarov, A.N. The Case of Intoxication with the Bite of the Gray Monitor Lizard *Varanus*. *Izvestia Akademii nauk Turkmenskoi SSR. Seriya Biol. Nauk* **1987**, *598*, 615. (In Russian)
47. Ballard, V.; Antonio, F.B. *Varanus griseus* (Desert Monitor) Toxicity. *Herpetol. Rev.* **2001**, *32*, 261.
48. Zima, Y.A. On the Toxicity of the Bite of the Caspian Desert Monitor Lizard (*Varanus griseus caspius*). *Biawak* **2019**, *13*, 115–118.
49. Sweet, S.S. Chasing Flamingos: Toxicofera and the Misinterpretation of Venom in Varanid Lizards. In *Proceedings of the 2015 Interdisciplinary World Conference on Monitor Lizards*; Cota, M., Ed.; Institute for Research and Development, Suan Sunandha Rajabhat University: Bangkok, Thailand, 2016; pp. 123–149.
50. Huang, T.-F.; Chiang, H.-S. Effect on Human Platelet Aggregation of Phospholipase A2 Purified from *Heloderma horridum* (Beaded Lizard) Venom. *Biochim. Biophys. Acta Lipids Lipid Metab.* **1994**, *1211*, 61–68. [[CrossRef](#)]
51. Utaincharoenso, P.; Mackessyn, S.P.; Miller, R.A.; Tusii, A.T. Complete Primary Structure and Biochemical Properties of Gilatoxin, a Serine Protease with Kallikrein-like and Angiotensin-Degrading Activities. *J. Biol. Chem.* **1993**, *268*, 21975–21983. [[CrossRef](#)]
52. Gorelov, Y.K. On the Toxicity of Saliva *Varanus griseus*. *Izvestia Akademii nauk Turkmenskoi SSR. Seriya Biol. Nauk* **1971**, *6*, 75–76. (In Russian)
53. Yang, D.C.; Dobson, J.; Cochran, C.; Dashevsky, D.; Arbuckle, K.; Benard, M.; Boyer, L.; Alagón, A.; Hendrikx, I.; Hodgson, W.C.; et al. The Bold and the Beautiful: A Neurotoxicity Comparison of New World Coral Snakes in the *Micruroides* and *Micrurus* Genera and Relative Neutralization by Antivenom. *Neurotox. Res.* **2017**, *32*, 487–495. [[CrossRef](#)]
54. Fry, B.G.; Lumsden, N.G.; Wuster, W.; Wickramaratna, J.C.; Hodgson, W.C.; Kini, R.M. Isolation of a Neurotoxin (Alpha-Colubritoxin) from a Nonvenomous Colubrid: Evidence for Early Origin of Venom in Snakes. *J. Mol. Evol.* **2003**, *57*, 446–452. [[CrossRef](#)]
55. Op den Brouw, B.; Coimbra, F.C.P.; Bourke, L.A.; Huynh, T.M.; Vlecken, D.H.W.; Ghezellou, P.; Visser, J.C.; Dobson, J.S.; Fernandez-Rojo, M.A.; Ikononopoulou, M.P.; et al. Extensive Variation in the Activities of Pseudocerastes and Eristicophis Viper Venoms Suggests Divergent Envenoming Strategies Are Used for Prey Capture. *Toxins* **2021**, *13*, 112. [[CrossRef](#)]
56. Lumsden, N.G.; Fry, B.G.; Manjunatha Kini, R.; Hodgson, W.C. In Vitro Neuromuscular Activity of ‘Colubrid’ Venoms: Clinical and Evolutionary Implications. *Toxicon* **2004**, *43*, 819–827. [[CrossRef](#)]
57. Harris, R.J.; Youngman, N.J.; Chan, W.; Bosmans, F.; Cheney, K.L.; Fry, B.G. Getting Stoned: Characterisation of the Coagulotoxic and Neurotoxic Effects of Reef Stonefish (*Synanceia verrucosa*) Venom. *Toxicol. Lett.* **2021**, *346*, 16–22. [[CrossRef](#)] [[PubMed](#)]
58. Jones, L.; Harris, R.J.; Fry, B.G. Not Goanna Get Me: Mutations in the Savannah Monitor Lizard (*Varanus exanthematicus*) Nicotinic Acetylcholine Receptor Confer Reduced Susceptibility to Sympatric Cobra Venoms. *Neurotox. Res.* **2021**, *39*, 1116–1122. [[CrossRef](#)] [[PubMed](#)]
59. Zdenek, N.C.; Harris, J.R.; Kuruppu, S.; Youngman, J.N.; Dobson, S.J.; Debono, J.; Khan, M.; Smith, I.; Yarski, M.; Harrich, D.; et al. A Taxon-Specific and High-Throughput Method for Measuring Ligand Binding to Nicotinic Acetylcholine Receptors. *Toxins* **2019**, *11*, 600. [[CrossRef](#)]
60. Harris, R.J.; Youngman, N.J.; Zdenek, C.N.; Huynh, T.M.; Nouwens, A.; Hodgson, W.C.; Harrich, D.; Dunstan, N.; Portes-junior, J.A.; Fry, B.G. Assessing the Binding of Venoms from Aquatic Elapids to the Nicotinic Acetylcholine Receptor Orthosteric Site of Different Prey Models. *Int. J. Mol. Sci.* **2020**, *21*, 7377. [[CrossRef](#)] [[PubMed](#)]
61. Harris, R.J.; Fry, B.G. Electrostatic Resistance to Alpha-Neurotoxins Conferred by Charge Reversal Mutations in Nicotinic Acetylcholine Receptors. *Proc. R. Soc. B* **2021**, *288*, 7–9. [[CrossRef](#)]
62. Harris, R.J.; Zdenek, C.N.; Debono, J.; Harrich, D.; Fry, B.G. Evolutionary Interpretations of Nicotinic Acetylcholine Receptor Targeting Venom Effects by a Clade of Asian Viperidae Snakes. *Neurotox. Res.* **2020**, *38*, 312–318. [[CrossRef](#)]
63. Youngman, N.J.; Harris, R.J.; Huynh, T.M.; Coster, K.; Sundman, E.; Braun, R.; Naude, A.; Hodgson, W.C.; Fry, B.G. Widespread and Differential Neurotoxicity in Venoms from the *Bitis* Genus of Viperid Snakes. *Neurotox. Res.* **2021**, *39*, 697–704. [[CrossRef](#)]
64. Modahl, C.; Mrinalini; Frietze, S.; Mackessy, S.P. Adaptive Evolution of Distinct Prey-Specific Toxin Genes in Rear-Fanged Snake Venom. *Proc. R. Soc. B Biol. Sci.* **2018**, *285*, 20181003. [[CrossRef](#)]
65. Harris, R.J.; Zdenek, C.N.; Harrich, D.; Frank, N.; Fry, B.G. An Appetite for Destruction: Detecting Prey-Selective Binding of α -Neurotoxins in the Venom of Afro-Asian Elapids. *Toxins* **2020**, *12*, 205. [[CrossRef](#)]
66. Heyborne, W.H.; Mackessy, S.P. Identification and Characterization of a Taxon-Specific Three-Finger Toxin from the Venom of the Green Vinesnake (*Oxybelis fulgidus*; family Colubridae). *Biochimie* **2013**, *95*, 1923–1932. [[CrossRef](#)]
67. Pawlak, J.; Mackessy, S.P.; Fry, B.G.; Bhatia, M.; Mourier, G.; Fruchart-gaillard, C.; Servent, D.; Stura, E.; Ménez, A.; Kini, R.M. Denmotoxin, a Three-finger Toxin from the Colubrid Snake *Boiga dendrophila* (Mangrove Catsnake) with Bird-specific Activity. *J. Biol. Chem.* **2006**, *281*, 29030–29041. [[CrossRef](#)]
68. Youngman, N.J.; Chowdhury, A.; Zdenek, C.N.; Coster, K.; Sundman, E.; Braun, R.; Fry, B.G. Utilising Venom Activity to Infer Dietary Composition of the Kenyan Horned Viper (*Bitis worthingtoni*). *Comp. Biochem. Physiol. Part C* **2021**, *240*, 108921. [[CrossRef](#)]

69. Youngman, N.J.; Zdenek, C.N.; Dobson, J.S.; Bittenbinder, M.A.; Gillett, A.; Hamilton, B.; Dunstan, N.; Allen, L.; Veary, A.; Veary, E.; et al. Mud in the Blood: Novel Potent Anticoagulant Coagulotoxicity in the Venoms of the Australian Elapid Snake Genus *Denisonia* (Mud Adders) and Relative Antivenom Efficacy. *Toxicol. Lett.* **2019**, *302*, 1–6. [[CrossRef](#)]
70. Cipriani, V.; Debono, J.; Goldenberg, J.; Jackson, T.N.W.; Arbuckle, K.; Dobson, J.; Koludarov, I.; Li, B.; Hay, C.; Dunstan, N.; et al. Correlation Between Ontogenetic Dietary Shifts and Venom Variation in Australian Brown Snakes (*Pseudonaja*). *Comp. Biochem. Physiol. Part C Toxicol. Pharmacol.* **2017**, *197*, 53–60. [[CrossRef](#)]
71. Daltry, J.C.; Wüster, W.; Thorpe, R.S. Diet and Snake Venom Evolution. *Nature* **1996**, *379*, 537–540. [[CrossRef](#)] [[PubMed](#)]
72. Zhang, M.; Fiedler, B.; Green, B.R.; Catlin, P.; Watkins, M.; Garrett, J.E.; Smith, B.J.; Yoshikami, D.; Olivera, B.M.; Bulaj, G. Structural and Functional Diversities among μ -Conotoxins Targeting TTX-Resistant Sodium Channels. *Biochem.* **2019**, *13*, 115–118. [[CrossRef](#)] [[PubMed](#)]
73. Wilson, M.J.; Yoshikami, D.; Azam, L.; Gajewiak, J.; Olivera, B.M.; Bulaj, G. μ -Conotoxins that Differentially Block Sodium Channels NaV1.1 through 1.8 Identify those Responsible for Action Potentials in Sciatic Nerve. *Proc. Natl. Acad. Sci. USA* **2011**, *108*, 10302–10307. [[CrossRef](#)] [[PubMed](#)]
74. Beck, D.D.; Lowe, C.H. Ecology of the Beaded Lizard, *Heloderma horridum*, in a Tropical Dry Forest in Jalisco, México. *J. Herpetol.* **1991**, *25*, 395–406. [[CrossRef](#)]
75. Hensley, M. Mammal Diet of *Heloderma*. *Herpetologica* **1949**, *5*, 5–6.
76. Chippaux, J.-P.; Amri, K. Severe *Heloderma* spp. Envenomation: A Review of the Literature. *Clin. Toxicol.* **2021**, *59*, 179–184. [[CrossRef](#)] [[PubMed](#)]
77. Abroug, F.; Souheil, E.; Ouanes, I.; Dachraoui, F.; Fekih-Hassen, M.; Besbes, L.O. Scorpion-Related Cardiomyopathy: Clinical Characteristics, Pathophysiology, and Treatment. *Clin. Toxicol.* **2015**, *53*, 511–518. [[CrossRef](#)]
78. Gilchrist, J.; Olivera, B.M.; Bosmans, F. Animal Toxins Influence Voltage-Gated Sodium Channel Function. In *Voltage Gated Sodium Channels*; Ruben, P.C., Ed.; Springer: Berlin/Heidelberg, Germany, 2014; pp. 203–229. ISBN 978-3-642-41588-3.
79. Cardoso, F.C.; Castro, J.; Grundy, L.; Schober, G.; Garcia-caraballo, S.; Zhao, T.; Herzig, V.; King, G.F.; Brierley, S.M.; Lewis, R.J. A Spider-Venom Peptide with Multitarget Activity on Sodium and Calcium Channels Alleviates Chronic Visceral Pain in a Model of Irritable Bowel Syndrome. *Pain* **2021**, *162*, 569–581. [[CrossRef](#)]
80. Dobson, J.; Yang, D.C.; op den Brouw, B.; Cochran, C.; Huynh, T.; Kurrupu, S.; Sánchez, E.E.; Massey, D.J.; Baumann, K.; Jackson, T.N.W.; et al. Rattling the Border Wall: Pathophysiological Implications of Functional and Proteomic Venom Variation between Mexican and US Subspecies of the Desert Rattlesnake *Crotalus scutulatus*. *Comp. Biochem. Physiol. Part C Toxicol. Pharmacol.* **2018**, *205*, 62–69. [[CrossRef](#)] [[PubMed](#)]
81. Martin-Eauclaire, M.F.; Ferracci, G.; Bosmans, F.; Bougis, P.E. A Surface Plasmon Resonance Approach to Monitor Toxin Interactions with an Isolated Voltage-Gated Sodium Channel Paddle Motif. *J. Gen. Physiol.* **2015**, *145*, 155–162. [[CrossRef](#)] [[PubMed](#)]